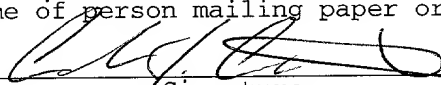


EXPRESS MAIL number: ET01403876505

Date of Deposit: SEPTEMBER 18, 2001

I hereby certify that this paper is being deposited with the United States Postal Service "EXPRESS MAIL Post Office to Addressee" service under 37 CFR 1.10 on the date indicated above and is addressed to the Assistant Commissioner for Patents; Washington, DC 20231.

ANDREW J. CURTIN
Name of person mailing paper or fee


Signature

=====

APPLICATION FOR UNITED STATES LETTERS PATENT

=====

Title: Computer Vision Depth Segmentation using
 Virtual Surface

Inventors: Yuri A. Ivanov,
 Alex P. Pentland, and
 Christopher R. Wren

Computer Vision Depth Segmentation using Virtual Surface

Field of the Invention

The present invention relates generally to the field of video analysis, and more particularly to segmenting depths in scenes observed by stereo video cameras.

5

Background of the Invention

10 The increasing availability of inexpensive video cameras and high-quality projection displays is providing opportunities for developing novel interfaces that use computer vision. These interfaces enable interactive applications that impose little constraint on a user and the environment. For example, the user can interact with objects in a scene without the need for a physical coupling between the user, the objects, and a computer system, as in more conventional mouse, or touch-based computer interfaces.

15 However, computer vision systems, with rare exceptions, are difficult to implement for applications where the visual appearance of objects and the scene change rapidly due to lighting fluctuations. Under dynamic lighting, traditional segmentation techniques generally fail.

20

The difficulty of implementation increases for interactive applications that use front-projected or rear-projected displays because the projector will illuminate foreground objects as well as the background. This makes color tracking and other appearance-based methods difficult, if not impossible to use.

25

By utilizing calibrated stereo cameras, it is possible to take advantage of 3-dimensional geometric constraints in the background to segment the scene using stereo analysis. Indeed, if the geometry of the background is known, then it becomes possible to determine a depth at every pixel in pairs of images, and compare these depths to the depths in images of a scene with static geometry, i.e., a scene without moving foreground objects. However, this process involves computing a dense depth map for each pair of images acquired by the stereo camera. This is computationally time consuming, and therefore unsuitable for applications that demand real-time performance.

Many prior art computer vision systems used for object recognition and motion analysis begin with some form of segmentation, see for example Friedman et al. “*Image segmentation in video sequences: A probabilistic approach*,” Thirteenth Conference on Uncertainty in Artificial Intelligence, 1997, Stauffer et al. “*Adaptive background mixture models for real-time tracking*,” Proc. of CVPR-99, pages 246–252, 1999, and Wren et al. “*Pfinder: Real-time tracking of the human body*,” IEEE Trans. on Pattern Analysis and Machine Intelligence, 19(7):780–785, 1997.

Typically, a real, tangible, physical background surface is measured over an extended period of time, and a 3D model is constructed using statistical properties of the measurements. The model is then used to determine which pixels in an input image are not part of the background, and therefore must be foreground pixels. Obviously, the background in the scene must remain relatively static for the segmentation to work, or at most, vary slowly with respect to geometry, reflectance, and illumination. For many practical applications that require natural interactions and natural user environments, these constraints are too restrictive.

Reliable segmentation for outdoor environments with a static geometry can be performed by using an explicit illumination model, see Oliver et al. “*A Bayesian computer vision system for modeling human interactions*,” Proceedings of ICVS99, 1999. There, the model is an eigenspace of images that describes a range of appearances in the scene under a variety of illumination conditions. Any different and unknown illumination dramatically degrades performance of the system, should it work at all. None of the above techniques accommodate rapidly changing lighting conditions, such as one would get when illuminating background and foreground objects with a dynamic, high-contrast projection display device.

Another class of prior art techniques take advantage of the geometry in the scene. For example, Gaspar et al., in “*Ground plane obstacle detection with a stereo vision system*,” International workshop on Intelligent Robotic Systems, 1994, describe constraints of a ground plane in order to detect obstacles in the path of a mobile robot.

Other methods employ special purpose multi-baseline stereo hardware to compute dense depth maps in real-time, see Okutomi et al. “*A multiple-baseline stereo*,” IEEE Trans. on Pattern Analysis and Machine Intelligence, 15(4):353–363, 1993. Provided with background disparity values, their method performs real-time depth segmentation, or “z-keying,” provided that the background does not vary, see Kanade “*A stereo machine for video-rate dense depth mapping and its new applications*,” In Proc. of Image Understanding Workshop, pages 805-811, 1995. However, the burden of computing dense, robust, real-time stereo maps is great.

Ivanov et al., in “*Fast lighting independent background subtraction*,” International Journal of Computer Vision, 37(2):199–207, 2000, describe a segmentation

method that first illuminates a physical background surface using a laser pointer. The location of the laser spot in stereo images is used to construct a sparse disparity map of the geometrically static, physical background surface. They use Delaunay triangulation to estimate neighborhood relationships anywhere in the 3D mesh. The disparity map is used to segment a foreground object from the background in real-time. As an advantage, a dense depth map is never explicitly computed. Instead, the pre-computed disparity map is used to rectify input images prior to direct image subtraction.

10 As a disadvantage, their method requires a time consuming measurement step with the laser pointer while stereo images are collected. This requires specialized equipment, and is error prone. Because the disparity map is modeled in the form of flat triangles, the method requires a high degree of human intervention when the surface is highly curved or otherwise irregular. In this case a sparse set of calibration points is insufficient because interpolation is ineffective in many areas.

15 In addition, their system requires a background surface that reflects laser light. This means that their method cannot be used to define virtual surfaces. Hereinafter, the term virtual surface means a surface that is geometrically defined in the real world and that is either tangible, i.e., a surface of a physical object, or some imaginary plane in space, not necessarily tangible, or only partially tangible.

20 This means their method cannot work for detecting objects in thin air, for example, a person entering through the virtual plane of an open doorway, or a ball falling through the virtual plane defined by a hoop. Nor, can their system deal with objects appearing from behind the background surface.

Moreover, their laser scanning is only practical for indoor scenes, and quite unsuitable for large scale outdoor scenes where it is desired to define depth planes geometrically, that in fact do not exist as tangible objects. Therefore, there still is a need for a robust depth segmentation technique that can operate in real-time on tangible and virtual surfaces in the physical world, at arbitrary scales.

Summary of the Invention

The present invention provides a system and method for segmenting a video of a scene so that various depths can be detected. The segmentation is insensitive to variations in lighting in the scene, and operates in real-time. A stereo camera is used to acquire a video of the scene. A disparity map for the scene is determined analytically. The disparity map is then used to detect regions in the scene that are not at predetermined depths.

More particularly, the invention facilitates identifying a location of an object in a physical scene with a stereo camera. A virtual surface is identified in the physical scene, and an approximate disparity set is constructed for the virtual surface. The stereo camera then acquires a main and a reference image of the scene. The reference image is warped according to the disparity set, and the warped image is subtracted from the main image to determine depth residuals of pixels in the main image. Pixels having a substantially non-zero residual are identified as lying on a surface of the object not coincident with the virtual surface. The decision threshold is set according to the level of noise in the images.

Furthermore, the invention may utilize an inherent thickness of the virtual surface, which called a virtual surface margin, to combine these virtual surfaces into

detection volumes as well as more complex computational structures. As a practical application, two such surfaces can be used to instantaneously detect contact between a foreground object, e.g., a pointer such as a finger, and a geometrically static background, e.g., a display surface. Due to the geometric nature of the segmentation, the detection of the touching is invariant to lighting, color, and motion in the scene, making the invention suitable for operations that require robust performance. The invention is therefore particularly applicable to interactive front- and back-projected displays.

10 **Brief Description of the Drawings**

Figure 1 is a block diagram of a depth segmentation system according to the invention;

Figure 2 is a flow diagram of the depth segmentation method according to the invention;

Figure 3 is a flow diagram of a process for constructing an approximate disparity map according to the invention;

Figures 4a-b are graphs of the disparity map of Figure 3; and

Figure 5 is a flow diagram of a process for determining disparity according to the invention.

Figure 6 is a diagram illustrating the relationship between a threshold, a residual, and a virtual surface margin.

Detailed Description of the Preferred Embodiment

System Structure

5

Figure 1 shows a depth segmentation system 100 according to our invention. Our system 100 includes a pair of stereo cameras 101-101', respectively a main camera M, and a reference camera R, aimed at a scene 102. The scene 102 includes a background object 103, for example, a table top or a game-board, and a foreground object 150, for example, a pointer or a game piece. The cameras 101-101' acquire pairs of images 104-104' that form a stereo video 105. The video 105 is analyzed by a processor 110.

10

15

20

The processor 110 is substantially conventional, including a microprocessor, memory, and I/O interfaces and devices, coupled to each other. The microprocessor executes operating system programs, and application programs implementing a fast depth segmentation (FDS) method 200 according to our invention, as described in greater detail below with reference to Figure 2. The system 100 can also include a projector 120 to illuminate the scene 102 with dynamically varying images.

System Operation

25

To estimate stereo disparity at a pixel location (x, y) 151 in the main image 104, it is necessary to locate the corresponding pixel (x', y') 152 in reference image 104'. An estimated stereo depth disparity $d(x, y)$ is a difference between these two pixel locations:

$$\mathbf{d}(x, y) = \begin{bmatrix} x' - x \\ y' - y \end{bmatrix}. \quad (1)$$

The depth disparity is used to estimate a depth to a location 153, for example, the top surface of a finger in the scene 102, corresponding to pixel (x, y) in the main image and pixel (x', y') in the reference image.

Method Overview

As shown in Figure 2, our FDS method 200 works in exactly the opposite way. The FDS method 200 takes as input the image pair 104-104', and an approximated disparity set (**D**) 160. In one embodiment, the set 160 represents a smooth, continuous surface, which may be physical or virtual.

As used herein, the term “virtual surface” broadly means some arbitrary surface in the **real** world that is either a physical surface of a physical object, partially coincident with a physical surface, or some imaginary plane in empty space, not necessarily tangible, or only partially tangible. For example, a real door frame can define the an imaginary, intangible plane of an open entry way. Additionally, it should be noted that “foreground” objects include **any** object **not** part of the background, including objects **behind** the virtual background surface 103.

The disparity set 160 is used to determine the estimated depth disparities $\mathbf{d}(x, y)$ between pixels in one image to corresponding pixels in the other image of the pair. A set **D** of all such disparities for all pixels of a given image pair is

$$\mathbf{D} = \begin{bmatrix} \cdot & \cdot & \cdot & \cdot \\ d(x_1, y_1) & d(x_2, y_2) & \dots & d(x_m, y_m) \\ \cdot & \cdot & \cdot & \cdot \end{bmatrix}. \quad (2)$$

The set \mathbf{D} 160 is used to warp 210 every reference pixel of the reference image 104', rectifying it with respect to the corresponding pixel of the main image 104 such that scene locations at predetermined depths will map to identical image locations. The warp operation is given by:

$$\mathbf{I}^w(x, y) = \mathbf{I}^r(x + \mathbf{D}^x(x, y), y + \mathbf{D}^y(x, y)), \quad (3)$$

where $\mathbf{D}^x(x, y)$, and $\mathbf{D}^y(x, y)$ are the x - and y - components of the disparity set \mathbf{D} at the location (x, y) .

After the reference image 104' is warped to correspond to the main image 104, a pixel-by-pixel subtraction 220 of the main image from the warped image yields a set \mathbf{S} 250 of depth residual values indicating differences between the two images, there is one depth residual value for every pixel.

$$\mathbf{S} = |\mathbf{I}^w(x, y) - \mathbf{I}(x, y)|. \quad (4)$$

In practice, some additional processing 230 is typically employed to remove noise and occlusion artifacts from the set 250. For example, all depth residuals smaller than a predetermined threshold \mathbf{T} 131 may be set to zero, and all other values set to one. This thresholding procedure yields a binary segmentation mask 240. Each bit in the mask 240 is either a zero or a one. Zero bits correspond to background locations in the scene, and one values correspond to foreground locations. The binary segmentation mask can be used to efficiently segment and track one or more foreground objects in a scene observed by the stereo cameras 101-101'.

Disparity Set Determination

In order to construct the approximated disparity set 160, and to perform the object segmentation, we provide two alternative analytical methods. We can determine the disparity set directly using known point-correspondences and smoothness constraints of the virtual surface 103. Alternatively, we can determine the disparity set from intrinsic and extrinsic parameters of the stereo camera pair 101-101'.

These two alternatives are now described in greater detail. In either case, we do not require the measurements of a complete continuous physical surface as in the prior art.

Direct Interpolation

As shown in Figure 3, we first acquire a sparse set m 301 of point correspondences from the cameras 101-101' in a calibration pair of images. In the case where the imaged surface is planar, e.g., when the object 103 is a chessboard, we can use the Intel Open Computer Vision Library chessboard finder functions to acquire these point correspondences by placing the chessboard at a desired depth plane, see “*Open Source Computer Vision Library Reference Manual*,” Intel Corporation, 2001 (hereafter “*Intel*”).

We use a smooth continuous approximation of a planar set m of point correspondences to determine the disparity set 160. For example, we construct the disparity set \mathbf{D} by a polynomial interpolation of the sparse set of point correspondences. A particular disparity, $\mathbf{d}(x, y)$ is approximated by the following linear system:

$$\mathbf{d}(x, y) = \Lambda \tilde{\mathbf{x}}(x, y), \quad (5)$$

where Λ is an unknown matrix of coefficients, and $\tilde{\mathbf{x}}(x, y)$ is a power expansion of $\mathbf{x} = [x, y]^T$, for example, a power of two expansions

$$\tilde{\mathbf{x}}(x, y) = \begin{bmatrix} x^2 \\ y^2 \\ xy \\ x \\ y \\ 1 \end{bmatrix}, \quad (6)$$

however, other powers can also be used.

Given the sparse set of m , we construct a matrix of powers:

$$\tilde{\mathbf{X}} = \begin{bmatrix} \cdot & \cdot & \cdot & \cdot \\ \tilde{x}(x_1, y_1) & \tilde{x}(x_2, y_2) & \dots & \tilde{x}(x_m, y_m) \\ \cdot & \cdot & \cdot & \cdot \end{bmatrix}. \quad (7)$$

An estimate of $\tilde{\Lambda}$ of the matrix coefficients Λ can be recovered by a least squares operation:

$$\tilde{\Lambda} = (\tilde{\mathbf{X}}\tilde{\mathbf{X}}^T)^{-1} \tilde{\mathbf{X}}^T \mathbf{D} \quad (8)$$

Then, we apply the linear system of equation 5 to each image location to determine the approximated disparity set.

15 An example approximated disparity set for a planar surface is shown in Figures 4a-b. Figure 4a shows the x displacements on the z -axis as a function of pixel location on the x -axis and y -axis, and Figure 4b the corresponding y displacements.

Analytic Technique

One application of the method and system of our invention is for the visual detection of the relationship between a foreground object 150 and an analytical surface, real or virtual. The analytic form of the surface allows us to derive an analytic expression for the disparity in a fairly straight-forward manner and thereby determine the disparity of any point on an arbitrary smooth surface.

We begin by introducing some notation used in the rest of this description. Let \mathbf{m} be a coordinate vector of a point in the image, $\tilde{\mathbf{m}}$ the point's homogeneous coordinates, \mathbf{M} a vector of coordinates of the imaged location on the surface in a “world” coordinate system, i.e., the scene 102, and $\tilde{\mathbf{M}}$ its homogeneous coordinates, respectively:

$$\mathbf{m} = \begin{bmatrix} u \\ v \end{bmatrix} \quad \tilde{\mathbf{m}} = \begin{bmatrix} u \\ v \\ 1 \end{bmatrix}, \text{ and} \quad (9)$$

$$\mathbf{M} = \begin{bmatrix} X \\ Y \\ g \end{bmatrix} \quad \tilde{\mathbf{M}} = \begin{bmatrix} X \\ Y \\ g \\ 1 \end{bmatrix}, \quad (10)$$

where g is some analytic function of X and Y in world coordinates, $g(X, Y)$.

Widely available camera calibration techniques, which are not the focus of our invention, and, therefore, are not described in any detail, *see, e.g., Intel* and O. Faugeras & Q. Luong, *The Geometry of Multiple Images*, MIT Press 2001, typically make available sets of values: the intrinsic camera parameters A , a matrix

R defining rotation, and a translation vector t that relates the physical coordinate system to the coordinate system at the optical center of the camera, \mathbf{O} . Under these transformations, the following relation maps locations in the scene to the locations of the pixels in the images as:

$$\tilde{\mathbf{m}} = A[R|t]\tilde{\mathbf{M}} \quad (11)$$

In general, the Z components of \mathbf{M} are determined by the value of some function of X and Y , i.e., $Z = g(X, Y)$. Without loss of generality, one application of our approach is to construct the disparity map set 160 for a virtual plane which has a constant value of $Z = C$ in the physical coordinate system.

As shown in Figure 5, our construction method proceeds in several steps. First, we transform the image coordinates of the image pixel 510 into the 3D camera coordinate system, \mathbf{r}_c :

$$\mathbf{r}_c = A^{-1}\tilde{\mathbf{m}}. \quad (12)$$

Second, we proceed with a transformation 520 to the real-world physical coordinates, i.e., $\mathbf{r}_c \rightarrow \mathbf{r}_w$:

$$\begin{aligned} \mathbf{r}_w &= R^{-1}(\mathbf{r}_c - \mathbf{t}) \\ &= R^{-1}[A^{-1}\tilde{\mathbf{m}} - \mathbf{t}] \\ &= (AR)^{-1}\tilde{\mathbf{m}} - R^{-1}\mathbf{t}. \end{aligned} \quad (13)$$

In order to determine the location of a point on the virtual surface that is imaged at location \mathbf{m} , we invoke the surface constraint, i.e., we identify a location in a plane for which $Z = g(X, Y)$. From a parametric equation of a ray \mathbf{L} passing from \mathbf{O}_w , the optical center of the camera expressed in real-world coordinates, through \mathbf{r}_w , the

real-world location of an image point, we solve for the disparity \mathbf{D} as follows in equations 14 through 20:

$$\mathbf{L}(s) = \mathbf{r}_w + s(\mathbf{r}_w - \mathbf{O}_w), \quad (14)$$

where s is a distance scaling factor specifying the length of the ray \mathbf{L} . The constant depth constraint results in the following equation:

$$L^z(s) = g(X, Y) = r_w^z + s(r_w^z - O_w^z), \quad (15)$$

where the superscript z denotes taking the Z component of the vector.

This allows us to solve for the scale parameter s of a location where the ray \mathbf{L} intersects a plane positioned at a distance $Z = g(X, Y)$ from the virtual background plane with a depth value of $Z = 0$;

$$s_g = - \frac{g - r_w^z}{r_w^z - O_w^z}. \quad (16)$$

Noting that $\mathbf{O}_w = -\mathbf{R}^{-1}\mathbf{t}$, we rewrite equation (16) explicitly to get the final form of the constraint on s :

$$s_g = - \frac{g + [\mathbf{R}^{-1}\mathbf{t}]_z}{[(\mathbf{A}\mathbf{R})^{-1}\tilde{\mathbf{m}}]_z}. \quad (17)$$

Therefore, a location of a point on the surface with depth $Z = g(X, Y)$ is determined by

$$\begin{aligned} \mathbf{M}_g &= \mathbf{r}_w + s_g(\mathbf{r}_w - \mathbf{O}_w). \\ &= (\mathbf{A}\mathbf{R})^{-1}[1 + s_g]\tilde{\mathbf{m}} \end{aligned} \quad (18)$$

With the set of calibration parameters A^r , R^r , and \mathbf{t}^r of the reference camera 101', we now determine 550 the pixel location \mathbf{m}^r in the image 104 of the reference camera 101' by

$$\tilde{\mathbf{m}}_g^r = A^r [R^r | \mathbf{t}^r] \mathbf{M}_g. \quad (19)$$

5

Finally, the disparity for the pixel at location \mathbf{m} in the main image 104 is determined 560 by

$$\mathbf{D} = \mathbf{m}_g^r - \mathbf{m}. \quad (20)$$

10 We perform this determination once for every pixel in the main image 104 in order to construct the disparity map 160.

Virtual Surface Margin and Virtual Volume

15

Figure 6 illustrates a real world situation that occurs for each pair of pixels in the stereo images 104-104' of Figure 1 near a virtual surface 600. Here, 601 and 601' label a bundle of light rays imaged by any given pair of pixels in corresponding cameras 101 and 101' respectively, that are related through the disparity map 160.

20

If there is a real surface coincident with the virtual surface 600 that is defined by the disparity map 160, then a pair of pixels 602 images the exact same patch of the surface. This is a case where pixel measurements are substantially identical, and any residual only represents imaging noise.

25

For the case where the real surface is slightly nearer or farther from the cameras than the virtual surface 600, pairs of pixels 603 image slightly different parts of the surface, and the pixel measurements differ slightly. Consequently, the residual is greater than in the above case.

5

As the real surface moves farther from the virtual surface, less overlap exists in a pair 604, until the case where a pair of pixels 605 image completely different patches of the surface, and the residual is dominated by properties, e.g., luminance and chrominance, of the surface rather than its geometry.

10

Therefore, for any given threshold T 231, noise, geometry, and surface properties combine to form a margin Δ surrounding the virtual surface 600. This virtual surface margin Δ means that the virtual surface 600, in the real world as imaged by the camera, does not have zero thickness. In fact, the virtual “surface” is imaged as a thin slice or virtual volume 610 with a thickness equal to the margin Δ . This means that by measuring the residuals and bitmaps from a set of virtual surfaces, and combining these results with Boolean operations, it is possible to perform more complex volumetric depth segmentation operations.

15

20 **Touch Application**

The invention enables a number of practical applications. In one application, the system 100 can be used as a touch-system. In this case, the pointer 150 is a user’s finger, or a stylus held by the user, and the system determines where on the surface the user is pointing at the object. The application of the process to the planar projection surface simplifies the calculations shown above, where the analytic form of the Z component of the imaged surface is $Z = g(X, Y) = C$, a constant. As stated

25

above, the effective surface does not need be the actual physical surface, but could also be some off-set virtual surface above the physical surface. Therefore, as an advantage, the user does not actually need to make physical contact with a target object. Bringing the pointer's tip close to the surface is sufficient to indicate a touching. Consequently, the system can be used with objects that are sensitive to touching, or should not be touched at all, i.e., where prior-art mouse, conductive or capacitive touch technologies cannot or should not be used.

To further enhance the interactive operability, the background object can be illuminated by a dynamic projector. The fact that the foreground object is also illuminated, perhaps by a high contrast image, which would confuse prior art vision system, is of no consequence. Thus, the system of our invention can be used for games, modeling, and system control applications.

In addition, the system is easily adapted to any type of object without requiring the physical modification or re-engineering of the targeted object to be touch enabled. The system can also be used to detect "penetration" of a virtual surface, for example, the entry of a person through an open door way. Pointing the stereo cameras at the door or any other "empty" space allows the invention to detect foreground objects entering and leaving the space.

For these applications, the cameras 101 are first calibrated for the selected surface, as above. Then, we construct the disparity map for the surface by setting $g(X, Y) = C = 0$ in equations (16) and (17), which induces a virtual plane that is coincident with the physical surface. In practice, a "virtual" surface somewhat near the physical surface can be marked as satisfying the constraint, even when the virtual surface is not strictly coincident with the physical surface. Areas that do not satisfy

the constraint are unambiguously part of the foreground because they are not in or near the plane of the physical surface, and, obviously, cannot be behind it if the surface is solid and opaque.

5 The actual processing executes two instances of the FDS method 200. A first instance detects foreground objects at the physical surface, and the second instance detects objects just above the physical surface, i.e., $g(X, Y) = C > 0$ in equations (16) and (17). The magnitude of the offset, that is, an offset threshold, can be determined by the specific application. For example, for a touch application C can
10 be set to about the width of a finger, or slightly greater. When the top surface of the finger coincides with C , i.e., the offset virtual surface, the real physical surface must have been touched.

Any implementation would also benefit from color calibration of the cameras 101-
15 101'. Being able to treat each color channel separately in the difference magnitude computation provides better discrimination, and therefore cleaner segmentation.

Our system performs depth segmentation maps in a substantially shorter time than approaches that use full stereo processing because the system takes advantage of
20 stereo disparity constraints in the environment. In addition, the system can also recover a measure of physical proximity between observed objects that would otherwise be difficult to do using prior art techniques.

This invention is described using specific terms and examples. It is to be
25 understood that various other adaptations and modifications may be made within the spirit and scope of the invention. Therefore, it is the object of the appended

claims to cover all such variations and modifications as come within the true spirit and scope of the invention.

11
12
13
14
15
16
17
18
19
20
21
22
23
24
25
26
27
28
29
30
31
32
33
34
35
36
37
38
39
40
41
42
43
44
45
46
47
48
49
50
51
52
53
54
55
56
57
58
59
60
61
62
63
64
65
66
67
68
69
70
71
72
73
74
75
76
77
78
79
80
81
82
83
84
85
86
87
88
89
90
91
92
93
94
95
96
97
98
99
100
101
102
103
104
105
106
107
108
109
110
111
112
113
114
115
116
117
118
119
120
121
122
123
124
125
126
127
128
129
130
131
132
133
134
135
136
137
138
139
140
141
142
143
144
145
146
147
148
149
150
151
152
153
154
155
156
157
158
159
160
161
162
163
164
165
166
167
168
169
170
171
172
173
174
175
176
177
178
179
180
181
182
183
184
185
186
187
188
189
190
191
192
193
194
195
196
197
198
199
200
201
202
203
204
205
206
207
208
209
210
211
212
213
214
215
216
217
218
219
220
221
222
223
224
225
226
227
228
229
230
231
232
233
234
235
236
237
238
239
240
241
242
243
244
245
246
247
248
249
250
251
252
253
254
255
256
257
258
259
260
261
262
263
264
265
266
267
268
269
270
271
272
273
274
275
276
277
278
279
280
281
282
283
284
285
286
287
288
289
290
291
292
293
294
295
296
297
298
299
300
301
302
303
304
305
306
307
308
309
310
311
312
313
314
315
316
317
318
319
320
321
322
323
324
325
326
327
328
329
330
331
332
333
334
335
336
337
338
339
340
341
342
343
344
345
346
347
348
349
350
351
352
353
354
355
356
357
358
359
360
361
362
363
364
365
366
367
368
369
370
371
372
373
374
375
376
377
378
379
380
381
382
383
384
385
386
387
388
389
390
391
392
393
394
395
396
397
398
399
400
401
402
403
404
405
406
407
408
409
410
411
412
413
414
415
416
417
418
419
420
421
422
423
424
425
426
427
428
429
430
431
432
433
434
435
436
437
438
439
440
441
442
443
444
445
446
447
448
449
450
451
452
453
454
455
456
457
458
459
460
461
462
463
464
465
466
467
468
469
470
471
472
473
474
475
476
477
478
479
480
481
482
483
484
485
486
487
488
489
490
491
492
493
494
495
496
497
498
499
500
501
502
503
504
505
506
507
508
509
510
511
512
513
514
515
516
517
518
519
520
521
522
523
524
525
526
527
528
529
530
531
532
533
534
535
536
537
538
539
540
541
542
543
544
545
546
547
548
549
550
551
552
553
554
555
556
557
558
559
560
561
562
563
564
565
566
567
568
569
570
571
572
573
574
575
576
577
578
579
580
581
582
583
584
585
586
587
588
589
590
591
592
593
594
595
596
597
598
599
600
601
602
603
604
605
606
607
608
609
610
611
612
613
614
615
616
617
618
619
620
621
622
623
624
625
626
627
628
629
630
631
632
633
634
635
636
637
638
639
640
641
642
643
644
645
646
647
648
649
650
651
652
653
654
655
656
657
658
659
660
661
662
663
664
665
666
667
668
669
670
671
672
673
674
675
676
677
678
679
680
681
682
683
684
685
686
687
688
689
690
691
692
693
694
695
696
697
698
699
700
701
702
703
704
705
706
707
708
709
710
711
712
713
714
715
716
717
718
719
720
721
722
723
724
725
726
727
728
729
730
731
732
733
734
735
736
737
738
739
740
741
742
743
744
745
746
747
748
749
750
751
752
753
754
755
756
757
758
759
760
761
762
763
764
765
766
767
768
769
770
771
772
773
774
775
776
777
778
779
780
781
782
783
784
785
786
787
788
789
790
791
792
793
794
795
796
797
798
799
800
801
802
803
804
805
806
807
808
809
810
811
812
813
814
815
816
817
818
819
820
821
822
823
824
825
826
827
828
829
830
831
832
833
834
835
836
837
838
839
840
841
842
843
844
845
846
847
848
849
850
851
852
853
854
855
856
857
858
859
860
861
862
863
864
865
866
867
868
869
870
871
872
873
874
875
876
877
878
879
880
881
882
883
884
885
886
887
888
889
890
891
892
893
894
895
896
897
898
899
900
901
902
903
904
905
906
907
908
909
910
911
912
913
914
915
916
917
918
919
920
921
922
923
924
925
926
927
928
929
930
931
932
933
934
935
936
937
938
939
940
941
942
943
944
945
946
947
948
949
950
951
952
953
954
955
956
957
958
959
960
961
962
963
964
965
966
967
968
969
970
971
972
973
974
975
976
977
978
979
980
981
982
983
984
985
986
987
988
989
990
991
992
993
994
995
996
997
998
999
1000
1001
1002
1003
1004
1005
1006
1007
1008
1009
1010
1011
1012
1013
1014
1015
1016
1017
1018
1019
1020
1021
1022
1023
1024
1025
1026
1027
1028
1029
1030
1031
1032
1033
1034
1035
1036
1037
1038
1039
1040
1041
1042
1043
1044
1045
1046
1047
1048
1049
1050
1051
1052
1053
1054
1055
1056
1057
1058
1059
1060
1061
1062
1063
1064
1065
1066
1067
1068
1069
1070
1071
1072
1073
1074
1075
1076
1077
1078
1079
1080
1081
1082
1083
1084
1085
1086
1087
1088
1089
1090
1091
1092
1093
1094
1095
1096
1097
1098
1099
1100
1101
1102
1103
1104
1105
1106
1107
1108
1109
1110
1111
1112
1113
1114
1115
1116
1117
1118
1119
1120
1121
1122
1123
1124
1125
1126
1127
1128
1129
1130
1131
1132
1133
1134
1135
1136
1137
1138
1139
1140
1141
1142
1143
1144
1145
1146
1147
1148
1149
1150
1151
1152
1153
1154
1155
1156
1157
1158
1159
1160
1161
1162
1163
1164
1165
1166
1167
1168
1169
1170
1171
1172
1173
1174
1175
1176
1177
1178
1179
1180
1181
1182
1183
1184
1185
1186
1187
1188
1189
1190
1191
1192
1193
1194
1195
1196
1197
1198
1199
1200
1201
1202
1203
1204
1205
1206
1207
1208
1209
1210
1211
1212
1213
1214
1215
1216
1217
1218
1219
1220
1221
1222
1223
1224
1225
1226
1227
1228
1229
1230
1231
1232
1233
1234
1235
1236
1237
1238
1239
1240
1241
1242
1243
1244
1245
1246
1247
1248
1249
1250
1251
1252
1253
1254
1255
1256
1257
1258
1259
1260
1261
1262
1263
1264
1265
1266
1267
1268
1269
1270
1271
1272
1273
1274
1275
1276
1277
1278
1279
1280
1281
1282
1283
1284
1285
1286
1287
1288
1289
1290
1291
1292
1293
1294
1295
1296
1297
1298
1299
1300
1301
1302
1303
1304
1305
1306
1307
1308
1309
1310
1311
1312
1313
1314
1315
1316
1317
1318
1319
1320
1321
1322
1323
1324
1325
1326
1327
1328
1329
1330
1331
1332
1333
1334
1335
1336
1337
1338
1339
1340
1341
1342
1343
1344
1345
1346
1347
1348
1349
1350
1351
1352
1353
1354
1355
1356
1357
1358
1359
1360
1361
1362
1363
1364
1365
1366
1367
1368
1369
1370
1371
1372
1373
1374
1375
1376
1377
1378
1379
1380
1381
1382
1383
1384
1385
1386
1387
1388
1389
1390
1391
1392
1393
1394
1395
1396
1397
1398
1399
1400
1401
1402
1403
1404
1405
1406
1407
1408
1409
1410
1411
1412
1413
1414
1415
1416
1417
1418
1419
1420
1421
1422
1423
1424
1425
1426
1427
1428
1429
1430
1431
1432
1433
1434
1435
1436
1437
1438
1439
1440
1441
1442
1443
1444
1445
1446
1447
1448
1449
1450
1451
1452
1453
1454
1455
1456
1457
1458
1459
1460
1461
1462
1463
1464
1465
1466
1467
1468
1469
1470
1471
1472
1473
1474
1475
1476
1477
1478
1479
1480
1481
1482
1483
1484
1485
1486
1487
1488
1489
1490
1491
1492
1493
1494
1495
1496
1497
1498
1499
1500
1501
1502
1503
1504
1505
1506
1507
1508
1509
1510
1511
1512
1513
1514
1515
1516
1517
1518
1519
1520
1521
1522
1523
1524
1525
1526
1527
1528
1529
1530
1531
1532
1533
1534
1535
1536
1537
1538
1539
1540
1541
1542
1543
1544
1545
1546
1547
1548
1549
1550
1551
1552
1553
1554
1555
1556
1557
1558
1559
1560
1561
1562
1563
1564
1565
1566
1567
1568
1569
1570
1571
1572
1573
1574
1575
1576
1577
1578
1579
1580
1581
1582
1583
1584
1585
1586
1587
1588
1589
1590
1591
1592
1593
1594
1595
1596
1597
1598
1599
1600
1601
1602
1603
1604
1605
1606
1607
1608
1609
1610
1611
1612
1613
1614
1615
1616
1617
1618
1619
1620
1621
1622
1623
1624
1625
1626
1627
1628
1629
1630
1631
1632
1633
1634
1635
1636
1637
1638
1639
1640
1641
1642
1643
1644
1645
1646
1647
1648
1649
1650
1651
1652
1653
1654
1655
1656
1657
1658
1659
1660
1661
1662
1663
1664
1665
1666
1667
1668
1669
1670
1671
1672
1673
1674
1675
1676
1677
1678
1679
1680
1681
1682
1683
1684
1685
1686
1687
1688
1689
1690
1691
1692
1693
1694
1695
1696
1697
1698
1699
1700
1701
1702
1703
1704
1705
1706
1707
1708
1709
1710
1711
1712
1713
1714
1715
1716
1717
1718
1719
1720
1721
1722
1723
1724
1725
1726
1727
1728
1729
1730
1731
1732
1733
1734
1735
1736
1737
1738
1739
1740
1741
1742
1743
1744
1745
1746
1747
1748
1749
1750
1751
1752
1753
1754
1755
1756
1757
1758
1759
1760
1761
1762
1763
1764
1765
1766
1767
1768
1769
1770
1771
1772
1773
1774
1775
1776
1777
1778
1779
1780
1781
1782
1783
1784
1785
1786
1787
1788
1789
1790
1791
1792
1793
1794
1795
1796
1797
1798
1799
1800
1801
1802
1803
1804
1805
1806
1807
1808
1809
1810
1811
1812
1813
1814
1815
1816
1817
1818
1819
1820
1821
1822
1823
1824
1825
1826
1827
1828
1829
1830
1831
1832
1833
1834
1835
1836
1837
1838
1839
1840
1841
1842
1843
1844
1845
1846
1847
1848
1849
1850
1851
1852
1853
1854
1855
1856
1857
1858
1859
1860
1861
1862
1863
1864
1865
1866
1867
1868
1869
1870
1871
1872
1873
1874
1875
1876
1877
1878
1879
1880
1881
1882
1883
1884
1885
1886
1887
1888
1889
1890
1891
1892
1893
1894
1895
1896
1897
1898
1899
1900
1901
1902
1903
1904
1905
1906
1907
1908
1909
1910
1911
1912
1913
1914
1915
1916
1917
1918
1919
1920
1921
1922
1923
1924
1925
1926
1927
1928
1929
1930
1931
1932
1933
1934
1935
1936
1937
1938
1939
1940
1941
1942
1943
1944
1945
1946
1947
1948
1949
1950
1951
1952
1953
1954
1955
1956
1957
1958
1959
1960
1961
1962
1963
1964
1965
1966
1967
1968
1969
1970
1971
1972
1973
1974
1975
1976
1977
1978
1979
1980
1981
1982
1983
1984
1985
1986
1987
1988
1989
1990
1991
1992
1993
1994
1995
1996
1997
1998
1999
2000
2001
2002
2003
2004
2005
2006
2007
2008
2009
2010
2011
2012
2013
2014
2015
2016
2017
2018
2019
2020
2021
2022
2023
2024
2025
2026
2027
2028
2029
2030
2031
2032
2033
2034
2035
2036
2037
2038
2039
2040
2041
2042
2043
2044
2045
2046
2047
2048
2049
2050
2051
2052
2053
2054
2055
2056
2057
2058
2059
2060
2061
2062
2063
2064
2065
2066
2067
2068
2069
2070
2071
2072
2073
2074
2075
2076
2077
2078
2079
2080
2081
2082
2083
2084
2085
2086
2087
2088
2089
2090
2091
2092
2093
2094
2095
2096
2097
2098
2099
2100
2101
2102
2103
2104
2105
2106
2107
2108
2109
2110
2111
2112
2113
2114
2115
2116
2117
2118
2119
2120
2121
2122
2123
2124
2125
2126
2127
2128
2129
2130
2131
2132
2133
2134
2135
2136
2137
2138
2139
2140
2141
2142
2143
2144
2145
2146
2147
2148
2149
2150
2151
2152
2153
2154
2155
2156
2157
2158
2159
2160
2161
2162
2163
2164
2165
2166
2167
2168
2169
2170
2171
2172
2173
2174
2175
2176
2177
2178
2179
2180
2181
2182
2183
2184
2185
2186
2187
2188
2189
2190
2191
2192
2193
2194
2195
2196
2197
2198
2199
2200
2201
2202
2203
2204
2205
2206
2207
2208
2209
2210
2211
2212
2213
2214
2215
2216
2217
2218
2219
2220
2221
2222
2223
2224
2225
2226
2227
2228
2229
2230
2231
2232
2233
22